A thermomechanical framework for reconciling the effects of ultraviolet radiation exposure time and wavelength on connective tissue elasticity

Goh KL[1 *], Chen SY[2], Liao K[3]

1 School of Mechanical and Systems Engineering, Newcastle University, Newcastle, UK

2 School of Chemical & Biomedical Engineering, Nanyang Technological University, Singapore

3 Mechanical Engineering Department, Khalifa University of Science Technology and Research, UAE

* Corresponding email: kheng-lim.goh@ncl.ac.uk

Running head: Effects of ultraviolet radiation on tissue elasticity

Keywords: elastic modulus; modulus of resilience; energy transfer; cross-linking; scission

Abstract

Augmentation of the mechanical properties of connective tissue using ultraviolet (UV) radiation—by targeting collagen cross-linking in the tissue at predetermined UV exposure time (t) and wavelength (λ)—has been proposed as a therapeutic method for supporting the treatment of structural-related injuries and pathologies. However, the effects of λ and t on the tissue elasticity, namely elastic modulus (E) and modulus of resilience (u_Y), are not entirely clear. We present a thermomechanical framework to reconcile the t and λ related effects on E and u_Y. The framework addresses (1) an energy transfer model to describe the dependence of the absorbed UV photon energy, ξ, per unit mass of the tissue on t and λ, (2) an intervening thermodynamic shear-related parameter, G, to quantify the extent of UV-induced cross-linking in the tissue, (3) a threshold model for the G versus ξ relationship, characterized by t_C—the critical t underpinning the association of ξ with G—and (4) the role of G in the tissue elasticity. We hypothesized that G regulates E (UV-stiffening hypothesis) and u_Y (UV-resilience hypothesis). The framework was evaluated with the support from data derived from tensile testing on isolated ligament fascicles, treated with two levels of λ (365 and 254 nm) and three levels of t (15, 30 and 60 min). Predictions from the energy transfer model corroborated the findings from a two-factor analysis of variance of the effects of t and λ treatments. Student's t-test revealed positive change in E and u_Y with increases in G—the findings lend support to the hypotheses, implicating the implicit dependence of UV-induced cross-links on t and λ for directing tissue stiffness and resilience. From a practical perspective, the study is a step in the direction to establish a UV irradiation treatment protocol for effective control of exogeneous crosslinking in connective tissues.

1 Introduction

The use of ultraviolet radiation (UV) has been extensively investigated as a therapeutic method for supporting the treatment of structural-related injuries and pathologies (Wollensak et al. 2005, Lanchares 2011, Fessel et al. 2012 and therein). The subject addresses the photochemical cross-linking reaction for augmenting the mechanical properties of load-bearing connective tissues—guided by the theory of radiation-induced reactions in polymers (Charlesby 1977, 1981). To a large extent, as the biophysical mechanisms underlying the effects of the key illumination parameters, namely UV exposure time (t) and wavelength (λ), are not well-established, the findings have at times been conflicting. Thus, the application remains controversial.

For instance, consider the following studies where the focus was on t or λ as the singly applied treatment. In these instances, the terms positive and negative changes respectively refer to the augmentation and diminution of the tissue mechanical properties. We note that positive changes have been demonstrated at λ = 370 nm for cornea (Lanchares 2011) and sclera (Wollensak & Spoerl 2004; Wollensak et al. 2005). Of course, the innate functional variation of tissues, such as tendons, at different anatomical locations of the body could influence the outcome of UV irradiation (Fessel et al. 2012). At a slightly higher λ (= 374 nm), whereas positive changes were also observed for tail tendon, there was no significant change for digital tendon even in the presence of riboflavin, a photosensitizer known to promote cross-linking (Fessel et al. 2012). As for t, whereas tendons subjected to prolonged exposure $t \geq 120$ min led to negative changes (Sionkowska & Wess 2004), the degree of positive changes at short exposure times varies among different studies. For examples of reports on short exposure times (e.g. t = 30 min), we note that Sionkowska & Wess (2004) have alluded briefly to the results of no appreciable

change in the UV-irradiated tail tendons with respect to the untreated controls but no crucial details on the experimental data were provided. On the other hand, relatively modest positive changes were observed in the UV-irradiated riboflavin-impregnated tail tendons with respect to the untreated controls (Fessel et al. 2012) but there were no reference to crucial tests on UV-irradiated photosensitizer-absent specimens which could provide for a more coherent understanding of how UV influences the tissue mechanical properties. Above all, the use of different λs and *t*s in previous studies has limited attempts to carry out a comprehensive analysis of the intrinsic variability of different tissues. Thus, one motivation for the present study is to present a general strategy to clarify the dependence of the effects of one factor on the level of the other factor

The second motivation for the present study is concerned with quantifying the modifications to the tissue elasticity by UV. In this instance, elasticity refers to the mechanical response of the tissue to a normal physiological loading regime before the yield point (Goh et al. 2008). Elastic modulus (*E*, otherwise referred to as stiffness), a material-related parameter, has been evaluated for UV-irradiated tendon (Sionkowska & Wess 2004, Fessel et al. 2012), cornea (Lanchares 2011) and sclera (Wollensak et al. 2005). Typically, *E* is defined through Hooke's law, based on the assumption of a liner model in the stress-strain curve—*E* is identified with the gradient of the elastic region, which lies in between the toe region and the yield point of the stress-strain curve. In practice, since the extent of linearity within this region is debatable, the approach for determining *E* differs in these studies. In one approach, the mean *E* was estimated to order of the magnitude of the slope connecting two extreme points of the elastic region (Sionkowska & Wess 2004; Lanchares 2011; Fessel et al. 2012). In another approach, *E* was set equal to the gradient at predetermined strain points,

namely 0.08 and 0.50, respectively. The inconsistent approaches reported in these papers do not lend to a straightforward comparative analysis of the *E*. Studies on the other material-related elastic parameters for quantifying the state of yielding, namely modulus of resilience (u_Y) and yield stress (σ_Y), are less established. Although the yield strength, in terms of yield force and σ_Y of the respective tail and digital tendons, have been reported (Fessel et al. 2012), comparing the effects of UV on the yield strength of these tissues is not straightforward because the parameters address different intrinsic mechanical properties: the yield force is a structural-related parameter whereas σ_Y is a material-related parameter.

Here, we present a thermomechanical framework to clarify the roles of t and λ in tissue elasticity in a consistent manner that allows the elastic parameters to be compared for a given set of t and λ. The thermomechanical framework addresses (1) an energy transfer model to account for the absorbed dose, i.e. UV photon energy per unit mass of the tissue (ξ), at different levels of t and λ, (2) a thermodynamic shear-related parameter, G, which quantifies the cross-link density in the tissue, (3) a threshold model for the G versus ξ relationship—characterized by t_C—underpinning the association of ξ with G, and (4) the role of G for directing the tissue elasticity. Hypotheses were proposed to evaluate the significance of the structure-property relationship, i.e. between G and the tissue elasticity. Data derived from *in vitro* experiment was used to validate the model.

2 Methods

2.1 Model description

The role of UV in tissue elasticity involves the targeting of molecules that are responsible for mechanical stress uptake in extracellular matrix (ECM) and the

absorption of the UV photon energy by the tissue (Chan 2010). In principle, the higher the UV energy (in other words, the smaller the λ) the greater is the attenuation of the photon energy in the tissue, all things being equal (Meller & Moortgat 1997). The extent of the attenuation, which varies from material to material, is quantified by the absorption cross-section of the target molecule, α (Fujimori 1966). In particular, these molecular targets undergo excitation, ionization, or molecular fragmentation (Fujimori 1966, Chan 2010). At the tissue level, the ξ depends on other factors, such as t (David & Baeyens-Volant 1978, Chan 2010). Applying the arguments derived from polymer studies to the biomacromolecules in the tissue (Charlesby 1977, 1981; Samoria & Valles 2004), the net effect of irradiation may be a combination of polymer chain cross-linking and scission reactions; how one reaction dominates the other depends on the tissue and the operating conditions. It is widely accepted that cross-linking reaction predominates at short exposure times (e.g. 30 min) which in turn contributes to the augmentation of the tissue mechanical properties (Lanchares 2011; Fessel et al. 2012). However, prolonged exposure (1-24 h) leads to chain scission predominance, e.g. peptide bond breaking by free radicals (Charlesby 1977, 1981; Miles et al. 2000; Rabotyagova et al. 2008), which then contributes to the diminution of the mechanical properties (Sionkowska & Wess 2004). Following the assumptions employed by Samoria and Valles (2004), we assume that cross-linking and scission are independent reactions, i.e. both reactions do not influence each other, and that they occur sequentially. Consequently, this allows us to establish a thermomechanical framework for cross-link formation in collageneous tissue at short exposure times, assuming that chain scission reaction is negligible. We begin with an energy transfer model for the dependence of ξ on t and λ. The electron density of connective tissue (η) is given by

$$\eta = 4\pi^2 \kappa m_e e^{-2} [v / \lambda]^2 \quad (1)$$

(Thiyagarajan & Scharer 2008), where v is the speed of light, m_e the mass of the electron, e the electron charge and κ the permittivity of the micro-environment in the tissue during irradiation. To order of magnitude, we can identify the κ for modelling connective tissue with that of water at T (300 K, room temperature); we then find that $\kappa \approx 709\times10^{-12}$ F/m. As pointed out earlier, to some extent, the α decreases with increasing λ (Meller & Moortgat 1997). For collagen, $\alpha \approx 1.2\times10^{-17}$ cm^2 per amino acid unit at λ = 194 nm (Fisher & Hahn 2004) and we would expect α to decrease when we extrapolate from the results at 194 nm to 254 nm and 365 nm. The dependence of α on λ may be estimated using

$$\alpha = \exp(A(\lambda) + B(\lambda)[T - T_0]), \quad (2)$$

where T is the absolute temperature (T_0 = 273 K, reference temperature) and $A(\lambda)$ and $B(\lambda)$ are linear polynomial expressions of λ (Meller & Moortgat 1997). For simplicity,

$$\begin{cases} A = a_0 + a_1\lambda \\ B = b_0 + b_1\lambda \end{cases} \quad (3)$$

where a_i and b_i (i = 0, 1) are constants (within designated range of λs) of the respective polynomial. To order of magnitude, we designate a_0 = -1, $a_1 = -1\times10^{-6}$, b_0 = 5 and $b_1 = -1\times10^{-1}$ (for the 220-330 nm range); evaluating *Eq.* (2) at λ = 254 nm we

find $\alpha \approx 1\times10^{-25}$ cm^2. Similarly, we designate a_0 = -0.5, a_1 = -5×10^{-5}, b_0 = 1×10 and b_1 = -1×10^{-1} (for the 330-400 nm range); evaluating *Eq.* (2) at λ = 365 nm yields $\alpha \approx$ 1×10^{-26} cm^2. A point source of intensity, I_0, is used to model the UV emission. Let r represents the pathlength of the UV photon from the source. The attenuated intensity (I_r) at r is estimated to order of magnitude by Beer-Lambert's law at the molecular scale. One then finds that

$$I_r = I_0 \exp(-\alpha\eta r) \tag{4}$$

(David & Baeyens-Volant 1978). Let ρ/μ represents the specific surface area of the specimen where ρ is the surface area and μ the mass of the test specimen. For the UV photons penetrating through the tissue specimen, the magnitude of ξ is written as the product of I_r, t and ρ/μ,

$$\xi = I_r t\rho / \mu . \tag{5}$$

Let ξ_C parameterizes the critical ξ required for the formation of (intra- and inter-molecular) cross-links of collagen; let t_C represents the critical t at $\xi = \xi_C$. We identify ξ_C with the criteria for establishing an appreciable effect on the tissue elasticity. Order of magnitude estimate for the total bond energy associated with collagen cross-links (between two peptide chains) per unit mass of the tissue puts ξ_C at 168 J/g (40 cal/g, Balmer 1982). Of note, the energy needed to create a cross-link is of order of magnitude $10^4/N_A$ cal (Balmer 1982); thus ξ_C is about 10^{21} times greater than the energy associated with a single cross-link. We stress the illustrative nature of

the threshold ξ_C and that the value may be refined to account for possible cross-linking in other ECM components such as elastin, which predominates in aorta (Bailey 2001). Finally we note that whereas t is explicitly expressed in *Eq.* (5), λ is implicitly expressed in I_r. In this instance, λ is explicitly expressed in η (*Eq.* (1)) which is an input parameter for *Eq.* (5) to determine I_r.

To develop our argument further, we apply a statistical (mechanical) theory based on the elasticity of a network of (cross-linked) long-chain molecules (**Fig. 1** A, B; Treloar 1975) to model tissue deformation (Lepetit 2007). Details of the formulation of the model are found in Appendix A. Briefly, for a tissue subjected to an external tensile load within the small strain regime from initial loading up to the yield point of the tissue, it follows that the nominal tensile stress (σ) developed in the tissue is related to the nominal tensile strain (ε) as

$$\sigma = G\{[\varepsilon+1]-1/[\varepsilon+1]^2\} \tag{6}$$

where G is a thermodynamic shear-related parameter given by

$$G = NkT\,, \tag{7}$$

N is the number of collagen macromolecule segments joined by cross-linkages in collagen macromolecules per unit volume of ECM involved in the deformation of the tissue and k the Boltzmann constant. Here, N is of the order of the density of cross-links. From *Eq.* (6), dimensional analysis of G yields J/m^3 which is also dimensionally equivalent to Pa. Note further that G may be regarded as an intervening factor for quantifying the contribution of cross-linking to the macroscopic shear-

related modulus. However, for consistency with *Eq*. (6), we shall use Pa (instead of J/m^3) for *G*. According to the quasi-linear viscoelastic theory—which addresses the hyperelasticity and time-dependence of tissues—*Eq.* (6) describes the hyperelastic component of the tissue mechanical response (Defrate & Li 2007 and therein). The time dependent component is not considered here because we are only concerned with loads applied in time-scales that are much shorter than its relaxation time (Goh et al. 2005).

To complement the argument for the statistical theory, we present a threshold model to describe the *G* versus ξ relationship, characterized implicitly by the t_C which underpins the association of ξ with *G*. In other words, when the tissue is irradiated to $t = t_C$, this signals the tipping point $\xi = \xi_C$ for triggering a change in *G* from the minimum value ($G_{\min}$) to the maximum value ($G_{\max}$). From a practical point of view, t_C may be estimated, to order of magnitude, from *Eq*. (5). As discussed in Appendix C by solving a logistic differential equation (Hansford & Bailey 1992, Sadkowsi 2000), we arrive at an expression for the threshold model,

$$G = c_1 / \{1 + \exp(-[\xi - \xi_C] / \Delta\xi)\} + c_2 \tag{8}$$

where $\Delta\xi$ is the duration for the increase in *G* from $G_{\min}$ to $G_{\max}$ and c_1 and c_2 are constants. *Eq.* (8) describes a sigmoidal dependence of *G* on ξ. Fitting *Eq.* (8) to the experimental data of *G* versus ξ enables the $\Delta\xi$ and c_1 and c_2 to be determined.

The relationship between σ and ε in *Eq.* (6) is modulated by *G* from the point of initial loading to the yield point of the tissue. This relationship describes the role of *G* for directing the elastic response of the tissue, parameterize by *E* and u_Y. We

hypothesized that G regulates the E (UV-stiffening hypothesis) and u_Y (UV-resilience hypothesis). We outlined a strategy for validating the framework: (1) establish consistency in the prediction of ξ_C from both the energy transfer and threshold models; (2) test the hypotheses by evaluating the relationships of G versus E and u_Y, respectively, where G, E and u_Y are derived from experiment based on *in vitro* mechanical testing of ligament fascicles. For practical implementation of the thermomechanical framework, the energy transfer model is used to evaluate ξ at the specified values of t and λ.

2.2 Sample preparation

Individual fascicles were teased out from an anterior cruciate ligament (ACL), which was excised from a bovidae (sheep) hind limb within two hours of slaughter at a local abattoir, following a procedure reported elsewhere (Hirokawa & Sakoshita 2003). The fascicles were irradiated in the chamber (12.7 (H) × 30.5 (W) × 25.4 (D) cm) of a UV machine (Ultraviolet Crosslinkers CL-1000, UVP) at a fixed λ by five discharge-type tubes (8 Watt/tube) located on the chamber roof. To minimize dehydration, fascicles were submerged in phosphate buffer saline (PBS; pH 7.2) in a glass petri-dish; the dish was placed on the chamber floor at approximately 30.5 cm away from the middle discharge tube. A preset UV intensity of 0.06 $J.cm^{-2}min^{-1}$ was used. The treatment combinations involved six groups of fascicles based on a factorial arrangement of two levels of λ (365 and 254 nm) and three levels of t (15, 30 and 60 min). Here, the λs were selected to address the extreme regions of the UV spectrum (Rabotyagova et al. 2008); the range of t was selected so that the upper limit encompassed the largest t value noted for effective augmentation of the tissue mechanical properties (Fessel et al. 2012, Lanchares 2012). A control group (untreated) was established for the

purpose of comparison. Fifteen specimens (fascicles) were prepared for each group; a total of 105 specimens were prepared according to the three levels of *t*, two levels of λ and the control group.

2.3 Mechanical testing and microscopy

Details concerning the experimental procedure for mechanical testing and the derived mechanical parameters have been reported elsewhere (Goh et al. 2008, 2012). All specimens were stretched, while submerged in PBS (pH 7.2) in a petri dish at room temperature, at the displacement rate of 0.06 mm/s (Goh et al. 2008, 2012) to rupture using a custom-built horizontal tensile test rig (Sensorcraft Technology Pte Ltd). The rig was mounted onto the stage of an inverted microscope (TS100, Nikon) for observing the specimen during the test.

Typical profiles of the σ versus ε curve for the fascicles from the control group and a UV treated group are shown in **Fig. 1** C. Of note, only the tests where specimens broke within the central region were identified as successful measures of the mechanical parameters, namely E and u_Y. To determine E for each treatment combination, a fifth order polynomial equation was used to fit the σ-ε data points (of each sample) from the origin to the maximum stress point M (Derwin & Soslowsky 1999). The E defines the gradient (i.e. a tangent modulus) at the point of inflexion (i.e. Y) or otherwise known as the yield point (Goh et al. 2012); the σ and ε at Y correspond to the σ_Y and the yield strain, ε_Y, respectively. The modulus of resilience (u_Y) was calculated from the area under the plot of σ versus ε, from $\varepsilon = 0$ to ε_Y (Goh et al. 2012). Finally, *Eq.* (6) was fitted to the experimental dataset of σ-ε from $\varepsilon = 0$ to ε_Y to determine G.

Images of intact and ruptured fascicles were acquired from a scanning electron microscope (SEM; JSM-6390LA, JEOL). These images were analyzed to identify morphological differences implicating UV modifications of the tissue elasticity. All fascicles were coated with platinum using a coating machine (JFC-1600, JEOL) for 60 s at 20 mA before they were viewed using the SEM.

2.4 Statistical analysis

Experiments were conducted with all the six treatment combinations of the two factors. The tensile test data were analyzed using statistical software (Minitab, version 14, Minitab Inc.). Two-factor analysis of variance (ANOVA) was applied to fit the general linear model to the data to evaluate the main effects and interaction between t and λ. The zero level (controls) was not considered in order to avoid errors arising from repetitive data, i.e. using measurements from the same group. Accordingly, where interactions were significant and the main effects were not significant, one-way ANOVA was carried out to investigate the masking of the main effects of that particular parameter at the specific level of the other parameter. Two-sample t-test was used to investigate the UV-stiffening and UV-resilience hypotheses by assessing the significance in the difference between the respective elastic parameter at different levels of G; the analysis included data from the controls. The P value < 0.05 was used as the basis for the conclusion of significant difference. All results were reported as mean ± standard error of the mean unless indicated otherwise. The mean values of the respective elastic parameters and G, at each level of t and λ, were used to construct the interaction plots. To plot the main effects of λ (or t) of the respective elastic parameters and G, we used a representative value equal to the mean value over all t (or λ) levels at each λ (or t) level.

3 Results

3.1 Microscopic analysis

Overall, the macroscopic morphology of the fascicles from the control and UV treated groups revealed no discernible variation in the degree of opacity and the macroscopic crimp pattern (**Fig. 2** A). There was also no appreciable variation in the failure pattern for the control and UV treated groups. In general the failure dynamics involved delamination of the fibril bundles, leading to bundle sliding and pull-out (**Fig. 2** B). Similarly, SEM images revealed no discernible variation in the microscopic morphology of the fascicles among the control and UV treated groups. Typically, each fascicle featured numerous bundles (10 μm thick) of fibrils (**Fig. 2** C-D). Examination of the microstructure of ruptured fascicles at the bundle and fibril hierarchical levels revealed no appreciable variation in the failure patterns among the control and UV treated groups; all fascicles exhibited (1) bundle delamination, (2) fibril delamination (for fibrils lining the surface of the bundles), (3) bridging of the partially ruptured sites of the bundles by fibrils. Overall, the failure patterns of the ACL fascicles were strikingly similar to those of other load-bearing tissues (Goh et al. 2012). Although we have shown that short exposure time may not lead to visible changes in the tissue, prolonged irradiation (≥ 120 h) is expected to alter the surface morphology as well as the fracture morphology of the tissue (Sionkowska & Wess 2004)

3.2 Main effects and interactions

Results from the two-factor ANOVA indicated strong evidence for interactions between λ and t having an effect on the thermodynamic shear-related parameter, G (P = 0.003), and on the elastic parameters, E (P = 0.001) and u_Y (P = 0.013). For

informational purpose, interaction plots for the respective G, E and u_Y are shown in **Fig. 3** (left sub-panel).

The plots of the main effects of λ and t on the G, E and u_Y are shown in **Fig. 3** (right sub-panel). Significant effects were observed for G versus λ and E versus λ, suggesting that G and E were sensitive to λ. However, the significant effects of the interactions of λ with t on G, E and u_Y necessitated further analysis (see following paragraph) using one-way ANOVA to investigate the masking of the main effects of the factor which yielded no significant effects.

For the non-significant main effects in the presence of interaction, our findings on the influence of the factor (which yielded no significant variation) at the fixed level of the other are as follows. Significant variations were observed for (1) G with respect to t at the level of λ = 365 nm (P = 0.009), but not 254 nm (P = 0.341); (2) E with respect to t at the level of λ = 365 nm (P = 0.004) but not 254 nm (P = 0.192); (3) u_Y with respect to t at λ = 365 nm (P = 0.041; marginal) but not 254 nm (P = 0.107); (4) u_Y with respect to λ at the level of t = 30 min (P = 0.041) and 60 min (P = 0.041) but not at 15 min (P = 0.133). Of note, adding the controls to the above (main effects and interactions) analysis would not alter these conclusions.

Thus, the variations in the E and u_Y with respect to t were significant at λ = 365 nm but not at λ = 254 nm. Similar conclusion applies to the G. In all the cases, positive change was observed at t = 30 and 60 min. On the basis of these findings, in the next section we discuss how the thermomechanical framework is applied to reconcile the t and λ related effects on the elastic parameters.

3.3 Model validation

We begin with an analysis to provide estimates of I_r and ρ/μ for use in *Eq.* (5) to predict ξ. *Eq.* (1) predicts that increased λ results in decreased η. For this simplified treatment, substituting λ = 254 nm into *Eq.* (1) yields $\eta \approx 1.4\times10^{24}$ cm^{-3}; at λ = 365 nm, we find that $\eta \approx 6.7\times10^{23}$ cm^{-3}. Thus, η decreases by one order of magnitude when λ increases from 254 nm to 365 nm. We note that the value of η for air (Thiyagarajan & Scharer 2008) is about two to three orders of magnitude lower than those predicted for tissue; our estimates are not unrealistic given ECM in tissue is regarded as an example of composites comprising a mixture of solid (collagen) and liquid (hydrated proteoglycan(PG)-rich) phases (Goh et al. 2005; Quinn & Morel 2007). In fact, we can identify these estimates of η as the upper bounds for the tissue. To order of magnitude, $I_0 \approx 6000\times10^{-5}$ J.cm^{-2}min^{-1} (preset UV intensity) and $r \approx 13$ cm (height of the chamber); substituting these estimates of η, r and I_0 into *Eq.* (4) leads to $I_r \approx 990\times10^{-5}$ J.cm^{-2}min^{-1} (λ = 254 nm) and 5500×10^{-5} J.cm^{-2}min^{-1} (λ = 365 nm). Noting that $\mu \approx 0.05$ mg and the magnitude of ρ is of the order of the thickness of the fascicle (7.5×10^{-3} cm) times the sample length (1.0 cm), i.e. $\rho \approx 7.5\times10^{-3}$ cm^2, we find $\rho/\mu \approx 150$ cm^2/g.

Estimates of ρ/μ and I_r are substituted into *Eq.* (5) to compute ξ. We evaluated ξs for the six treatment combinations of the two factors, λ and t; the results are listed in Table 1. By inspection, at the level of λ = 254 nm, the values of ξ at t = 15, 30 and 60 min are all smaller than ξ_C, suggesting that the energy absorbed by the tissue is not sufficient to establish an appreciable effect on the tissue elasticity, corroborating the experimental findings of no significant changes in G, E and u_Y. At the level of λ = 365 nm (also see **Fig. 4 A**), the value of ξ at t = 15 min is smaller than ξ_C but the values

of ξ at t = 30 and 60 min are larger than ξ_C, suggesting that the cross-linking reaction at λ = 365 nm predominates within 15 to 30 min. Indeed, *Eq.* (5) predicts that $t_C \approx 20$ min at $\xi = \xi_C$, Altogether these predictions corroborated the experimental findings of positive changes in G, E and u_Y from t = 30 to 60 min.

According to the reports published by the manufacturer (Ultraviolet Crosslinker CL-1000, UVP), the UV spectral chart for the 254 nm bulb reveals an extremely narrow peak centered at around 254 nm (unfiltered). For the 365 nm bulb, the UV spectral chart reveals a broad (somewhat normally distributed) spectrum with a peak value centered at about 365 nm. To address the effects of the broad distribution of λ values on the model prediction, we have carried out a sensitivity analysis of the predicted t_C to λ at 330 nm and 375 nm, which correspond to the respective lower and upper limits of the full-width half maximum of the spectral distribution. Our calculations reveal that $t_C \approx 21$ min at λ = 330 nm and $t_C \approx 20$ min at λ = 375 nm; this suggests that λ has a marginal effect on the predictions of t_C.

Focusing on the main effects of ξ on G at λ = 365 nm (section 3.2), we have carried out an assessment of the sensitivity of the threshold model (*Eq.* (8)) for describing the experimental data of G versus ξ. Within experimental error, substituting $\Delta\xi$ = 1.3 J/g and 2.2 J/g into *Eq.* (8) leads to curves representing two extremes of the threshold model (**Fig. 4** B). One extreme ($\Delta\xi$ = 1.3 J/g) predicts a lower bound (≈ 166.6 J/g) for ξ_C whereas the other extreme ($\Delta\xi$ = 2.2 J/g) predicts an upper bound (≈ 190.2 J/g) for ξ_C. This has an important and immediate consequence: the value of ξ_C (= 168 J/g, section 2.1) adopted by the energy transfer model falls in between the two extremes.

Remarkably, both extremes lead to similar results for G_{max} (≈ 130.1 MPa) and G_{min} (≈ 63.8 MPa). Let $\Delta G = G_{max} - G_{min}$; numerically, we find $\Delta G \approx 67.3$ MPa.

On the basis of the findings of the main effects and interactions (section 3.2), data from the controls and UV-treated (λ = 365 nm) specimens were analyzed further to test the UV-stiffening and UV-resilience hypotheses. The strategy involved investigating the significant difference between the mean values of the respective elastic parameter at G_{min} and G_{max}. One way to approach this was to designate G_{min} with the data combined from the t = 15 min group and controls for the respective E and u_Y since statistical analysis revealed that the mean values of the respective parameter from the controls and t = 15 min group were not significantly different (section 3.2); similar arguments were applied to designate G_{max} with the data combined from the t = 30 min and 60 min groups of the respective elastic parameter. Finally, two-sample t-tests of the respective E and u_Y at the lower and upper levels of G yielded the following results: (1) the mean values of E, i.e. (231.0 ± 24.0) MPa and (485 ± 52) MPa, at G_{min} and G_{max}, respectively, were significantly different (P < 0.001; **Fig. 5** A), (2) the mean values of u_Y, i.e. (0.5 ± 0.1) MPa and (1.3 ± 0.2) MPa, at G_{min} and G_{max}, respectively, were also significantly different (P < 0.01; **Fig. 5** B). Thus, there is evidence for a (positive) difference in the respective E and u_Y with changes in G.

4 Discussion

4.1 UV-induced cross-links direct tissue stiffness and resilience

We thus see that the statistical analysis indicates support for the UV-stiffening hypothesis that holds that G regulates E. There are, however, important distinctions underlying the strategies for evaluating G and E, from the point of view of

interpreting the experimental data (σ, ε). In particular, E describes the response of the tissue to the change in the tensile stress per unit strain at the state associated with the yield point of the σ-ε curve. This may be viewed as an ad hoc modification of the elastic modulus which is defined through Hookes' law, based on the assumption of a linear model in σ and ε (as pointed out in section 1). This becomes clear when we consider that throughout ECM, in due proportion down to a very fine scale, the bulk of the collagen molecules would have been elastically (maximally) stretched to the limit as the tissue deforms towards the yield point, and consequently the ε is very nearly linearly proportional to the σ. Thus E reflects the tensile state of the deformed molecules—E manifests as the force (F) acting to overcome the interactions on the individual segments of collagen macromolecules per unit displacement (U). (Recall a segment refers to the portion of the macromolecule between successive points of cross-linkage, section 2.1.) On the other hand, G defines the overall profile of the σ-ε curve from the origin to the yield point. This model (*Eq.* (6)) is linear in the parameter G although it is not linear in σ and ε. With hindsight, it can be appreciated that the deformation of the collagen molecular network is predominated by molecular sliding from the relaxed state (i.e. at the origin of the σ-ε curve) to a fully stretched state (i.e. at the yield point) and thus G reflects the state of shear throughout ECM. How then does G regulate E? We note that the structural stiffness of a segment, F/U, is of the order of $[E_c a_c / L_0]$ (Gautieri et al. 2009), where E_c is the elastic modulus, a_c the average cross-sectional area and L_0 the average length of the segment. However, L_0 and the corresponding (average) mass of the segment (M) depend on N. As N increases within a collagen macromolecule, L_0 decreases, and consequently, M decreases, all things being equal. Extending the structure-property relationship to UV-irradiated tissue, starting with the relationship $G = NkT$ (*Eq.* (7)), one immediate and

important consequence is that only when a sufficient number of UV-induced cross-links (i.e. N) is present will the process proceed with an increase in G, i.e. from $G_{\min}$ to $G_{\max}$, and contribute to the positive increase in E. Now,

$$N = \beta N_A / M \tag{9}$$

(Treloar 1975), where β is the tissue density and N_A the Avogadro constant. For simplicity, rather than referring to L_0 (which is explicit in $[E_c a_c / L_0]U$), we look to M which is not only explicitly expressed in *Eq.* (9) but also implicit in *Eq.* (7). Thus, we find that G is inversely proportional to M. To address the structure-property relationship, a crucial question is what would be a possible relationship between E and G. According to Chalesby (1977), E is of the order of $3\beta N_A kT / M$, or simply $3G$ (according to *Eq.* (7) and (9)). Consequently, in this simplified treatment

$$E = \begin{cases} 3G_{\min} & \text{if} \quad \xi < \xi_C \\ 3G_{\max} & \text{if} \quad \xi \geq \xi_C \end{cases} . \tag{10}$$

Eq. (10) is also consistent with the general observation that the magnitude of E is approximately three times that of G (**Fig. 5** A).

The resilience, u_Y, is related to the energy (work of yielding) needed to cause cross-links to yield. This corresponds to the situation where the relationship between the force of interaction (associated with the cross-link between two atoms) versus the atomic displacement departs from linearity resulting in a state of force saturation (Buehler 2006). From a structure-property relationship point of view, physically, u_Y measures the extent (or depth) of the mechanical disturbance into the tissue fine

structure during the yielding process. Note further that statistical analysis (section 3.3) lends support to the UV-resilience hypothesis which holds that G regulates u_Y—in particular a step-wise increase in G contributes to an increase in u_Y. Since the strength and energy of the cross-links remain the same, it can only mean that a high u_Y reflects a greater depth of disturbance into the tissue fine structure below the surface. In the presence of an increased number of cross-links, when any one of the bonds yields during the process of disturbance, then the energy needed to cause yielding throughout a cross-section of the tissue increases.

4.2 Effectiveness of UV for cross-linking in the presence of photosensitizers

Studies on the effectiveness of UV for cross-linking have been well-documented for engineering collagen biomaterials (Chan 2010 and therein). As pointed out in section 1, UV photosensitizers such as riboflavin—a vitamin B2 compound—are used to promote cross-linking. Riboflavin is thought to participate in the crosslinking reaction via the indirect mechanism, i.e. the production of oxygen free radicals, without consuming themselves in the reaction (Chan 2010). When considering the effects of photosensitizers (Chan 2010), in the spirit of Charlesby's UV argument describing the radiochemical cross-link efficiency (Charlesby 1977, 1981), we can introduce a parameter at the macroscopic level known as the radiomechanical photosensitizer efficiency (Ω). It follows that Ω may be estimated, to order of magnitude, by the ratio of G of the UV-irradiated photosensitizer-impregnated specimens to that of UV-irradiated photosensitizer-absent specimens.

Table 1 lists the studies involving the use of riboflavin in tissues derived from animal models such as equine superficial digital flexor tendon (EDT, Fessel et al. 2012), rat tail tendon (RTT, Fessel et al. 2012), porcine cornea (PC, Lanchares 2011), rabbit

sclera (RS, Wollensak et al. 2005) and as well as human sclera (HS, Wollensak & Spoerl 2004). We highlight these studies to emphasize the broader applicability of the thermomechanical framework to other tissues; Appendix D examines the analysis of ξ of these tissues in detail. In the ξ column of Table 1, we identify the net energy absorbed by the respective riboflavin-impregnated tissues with $\Omega I_r t\rho/\mu$ to consistency with *Eq*. (5). For practical purpose—given *G* is not known but *E* is usually reported—in these instances, we quantify Ω using *E* in place of *G* which follows from the UV-stiffening hypothesis. We consider the RTT and EFT study of Fessel et al. (2012) for the purpose of illustration. The study revealed that the *E* of UV-irradiated riboflavin-impregnated RTT is about 1.2 times higher than that of the (untreated) controls. In section 1 we have pointed out that this increase is relatively modest. Also, as there is no reference to the *E* of UV-irradiated photosensitizer-absent RTT a conservative estimate places the *E* at equal to that of the controls—this is not an unrealistic estimate given the *E* is expected to lie in between that of the control and the treated specimen. More importantly, these estimates of *E* allow us to establish an upper bound for the Ω of the RTT specimens. It follows that Ω is of the order of the ratio of the *E* of UV-irradiated photosensitizer-impregnated RTT to that of UV-irradiated photosensitizer-absent RTT, giving Ω = 1.2. Thus the ξ is of the order of $\Omega I_r t\rho/\mu \approx$ 701 J/g—the presence of riboflavin can contribute to an increase in *E* because it leads to a net energy absorbed that is four times higher than that of ξ_C. As for the EFT study, since there is no significant change in the *E* of the riboflavin-impregnated EFTs (Fessel et al. 2012), we set Ω = 1. Thus the ξ of EDT is of the order of $\Omega I_r t\rho/\mu \approx$ 5 J/g—since this is two orders of magnitude less than ξ_C we

conclude that the UV energy absorbed in the photosensitizer-impregnated EFTs is insufficient to cause an appreciable effect on the tissue elasticity.

According to the energy transfer model, the concept of threshold—characterized implicitly by t_C—corroborates the experimental studies that the initial irradiation of tissues does not lead to an immediate augmentation of the tissue mechanical properties. In other words, only when a sufficient number of UV-induced cross-links is present will the process proceed with an increase in G, i.e. from $G_{\min}$ to $G_{\max}$, and contribute to the augmentation of the tissue elasticity (section 4.1). For the RTT study of Fessel et al. (2012), *Eq*. (5) predicts that $t_C \approx 9$ min (at $\xi = \xi_C$) for the photosensitizer-absent RTTs. In the presence of the photosensitizer (recall $\Omega = 1.2$, previous paragraph), we would expect a shorter critical time giving $t_C / \Omega \approx 9/1.2 \approx 7$ min. Although the reduction is marginal, erring on the side of caution, our findings suggest that setting $t = 10$ min should suffice to promote an appreciable increase in the E instead of $t = 30$ min as reported by the authors but this remains to be confirmed. For the EFT study (Fessel et al. 2012; recall $\Omega = 1.0$, previous paragraph), *Eq*. (5) predicts that $t_C \approx 1078$ min (at $\xi = \xi_C$) for the photosensitizer-impregnated EFTs which is 3.6 times longer than the t (= 30 min) implemented by the authors. Fessel et al. (2012) attributed the absence of a positive change to inadequate penetration of the UV into the equine tissue which is denser and larger than, e.g. RTT. Equivalently, our study suggests that a much longer irradiation time is needed in order to yield an appreciable increase in the E of EFT.

The prediction of t_C is important because most studies did not offer adequate justifications for the value of t used for promoting the augmentation of the tissue mechanical property. That said, the above arguments to quantify Ω for estimating the

effects of photosensitizers on t_C using the study of Fessel et al. (2012) apply also to the PC, RS and HS.

4.3 Model limitations

There are three important limitations that must be highlighted in weighing the implications of our findings. The first limitation concerns the model constants for computing ξ. Although there is a reasonable agreement between theory and experiment with regards to the predicted value of ξ for explaining the positive change in the elastic parameters, this should not be over interpreted since we normally have no independent measurements of the model constants, namely α, κ, η as well as the threshold ξ_C (= 168 J/g, which we have emphasized as illustrative, section 2.1). The fact that so many constants had to be used emphasizes the complexity of the estimated ξ. Of course, there are other alternative approaches for computing ξ as pointed out by Spoerl et al. (2012) and David & Baeyens-Volant (1977). In these instances, we note the argument presented by Spoerl et al. (2011) is only a crude approach (Appendix B); λ was not factored into the argument and it lends no insights into the physical mechanism at the molecular level. *Eq.* (20), proposed by David & Baeyens-Volant (1977) for determining ξ, involves only three parameters (Appendix B) but these will also require independent measurements plus the equation does not lend easily to insights into the physical mechanism at the molecular level.

The second limitation concerns the use of ACL as a tissue model to lend support to the thermomechanical framework, especially for the threshold model and for testing the UV-stiffening and UV-resilience hypotheses. To some extent, the ACL model may not be fully representative of other tissues (Table 1)—we would expect the collagen content to vary in many examples of connective tissue, because of innate

differences between species or specific load-bearing functions (Fessel et al. 2012). Therefore, applying the insights gain in this study, for instance the relationship between E and G (*Eq.* (10)), to other tissues may not be straightforward because the sensitivity of the thermomechanical framework to the variation in the collagen content and elastic properties has not been established. However the stress-strain response of ACL fascicles (Hirokawa & Sakoshita 2003; **Fig. 1** C) are strikingly similar to those of other skeletal tendons (Derwin & Soslowsky 1999; Goh et al. 2008; Fessel et al. 2009; Fessel et al. 2012; Goh et al. 2012). Additionally, the relevant limitations may be partly offset by the findings from the literature that yield consistency with the predictions from the thermomechanical framework, particularly the positive changes reported in the UV study on RTT (Fessel et al. 2012) and HS (Wollensak et al. 2005). Nevertheless, from a practical point of view, ligament meets the following essential criteria similar to other tendon fascicles (Derwin and Soslowsky, 1999; Fessel et al. 2012): one, it has a somewhat uniform anatomical structure along the axis and, henceforth, can be easily isolated and mechanically tested with high reproducibility; two, individual fascicles are possibly one hierarchical level above the structures of interest (i.e. collagen fibril). As pointed out by Fessel et al. (2009), satisfying these criteria then allows for a direct investigation of UV cross-links in collagen to mechanical properties (the structure–property relationship of ECM) since multi-scale (e.g. fascicles-fascicles) interactions at higher levels of the tissue hierarchy are excluded. Thus, it seems reasonable to adapt the statistical approach proposed by Lepetit (2007) to quantify G for studying the influence of UV-induced cross-links on the fascicle elasticity. One limitation of previous studies on the relationship between cross-links and mechanical properties of tissue is that quantification of the cross-links was not normally carried out for the same tissue that was designated for mechanical

testing (Derwin & Soslowsky 1999); our approach presents a possible strategy for overcoming this limitation. Finally, the key investigations of UV-irradiated tissues have been mostly done in tendon fascicles (Sionkowska & Wess 2004; Fessel et al. 2012) and the ACL model facilitates a more direct comparison with these studies.

The third limitation addresses the diminution of the mechanical properties of tissues subjected to prolonged UV exposure (Sionkowska & Wess 2004; Lanchares 2011). Table 1 lists the parameters of the studies on tissues subjected to prolonged UV exposure, namely RTT (Sionkowska & Wess 2004) and PC (Lanchares 2011). The RTT specimens were allotted to four *t* treatments (120, 240, 360 and 480 min) at λ = 254 nm (Sionkowska & Wess 2004). Lanchares (2011) treated the PCs (intact in the eye) with two levels of *t* (30 and 60 min) at λ = 370 nm. In both cases, we would expect the thermomechanical framework to support the outcome that indicates an appreciable increase on *E* since the predicted values of ξ (Table 1) are greater than ξ_C. Unfortunately, the *E* of RTT decreased with increasing *t*; the PC results revealed that 30 min irradiation significantly increases the *E* as compared to the controls but prolonging the irradiation to 60 min led to a significant decrease to the level of the controls. Altogether these suggest that short exposure time increases the *E* but prolonged exposure eventually leads to a reduction in *E*, and possibly even offsetting the *E* increase that arises from short exposure time. A crucial question is what implications arise if we propose, on the basis of these empirical findings, a second threshold, ξ_D, above which chain scission reaction of collagen macromolecules predominates. First, from the results of Sionkowska & Wess (2004) and Lanchares (2011), this places the value of ξ_D somewhat in between ξ_C and 1036 J/g. Second, the ACL findings that $\xi > \xi_C$ at *t* = 60 min (λ = 365 nm) needs further elaboration.

Revisiting the plot of G versus ξ (**Fig. 4** B), the upper level of the sigmoidal curve implicates the presence of an intermediate state for collagen macromolecules (Miles et al. 2000; Sionkowska & Wess 2004) whereby the cross-linking and scission reactions are probably proceeding at the same rate.

4.4 Conclusions

We have demonstrated a thermomechanical model that addresses (1) an energy transfer model for reconciling the dependence of λ and t on the UV energy absorbed in the tissue, (2) the prediction of the threshold for the predominance of the cross-link reaction and (3) the hypotheses that UV-induced cross-links regulate the tissue stiffness and resilience. This study adds new insights that may be applicable to the development of a general technique as part of clinical protocol for effective exogeneous crosslinking of tissues as well as minimizing the effects on the surrounding tissue (Wollensak & Spoerl, 2004; Wollensak et al., 2005).

Appendix A Statistical network theory of tissue elasticity

The key protein macromolecules that contribute to the load-bearing function of connective tissue (e.g. tendons, ligaments, cornea) are collagen, elastin, glycoproteins and, possibly, PG—collagen makes up the largest proportion of the tissue dry weight (Bailey 2001). The family of collagen comprises at least 28 different types (Kadler et al. 2007). Type I collagen is the most abundant member (it aggregates to form fibrous structures) in connective tissue (Orgel et al. 2011) and is also the most significant, particularly for its role in providing reinforcement to the hydrated PG-rich gel in ECM (Goh et al. 2005; Buehler 2006). According to the hierarchical architectural argument (section 4.3), collagen fibril is a semi-crystalline aggregate of type I collagen macromolecules (Orgel et al. 2011). While retaining its aggregate structure the fibril also aggregates with the other fibrils through PG associations (for instance) to form a fibril bundle (or otherwise known as a fibre) and bundles of these fibres form a fascicle. Many studies have highlighted the importance of the interaction of the PG with the collagen in regulating the tissue mechanical property, with the glycosaminoglycan sidechain of the PGs acting as mechanical cross-links for stress transfer between adjacent collagen fibrils (Scott 2003; Redaelli et al. 2004; Quinn & Morel 2007; Lewis et al. 2010, Orgel et al. 2011; Khoshgoftar et al. 2012) although experimental findings from a recent study have suggested otherwise (Rigozzi et al. 2013). Additionally, whether the fibrils and fibres have distinct surface molecular accessibilities (e.g. for PGs)—because of their different architectures—is still not clearly understood (Orgel et al. 2011). Nevertheless, given the dominance of collagen in most tissues, the focus of the discussion that follows is on the role of cross-link, in terms of its overall presence within the collagen molecular network, in tissue elasticity in the presence of UV. (Of note, this strategy predicts the stress versus

extension behavior, *Eq.* (19), of the tissue which applies to the situation at small extension when deformation begins from a relaxed state but inevitably overestimates the stress at large extension, i.e. beyond the yield point.) However, the strategy allows for further generalization to account for mechanical crosslinks (i.e. PGs) and we have targeted this for further study.

Consider ECM collagen macromolecules as networks of long molecules segmented at successive points of cross-linkage (inset in **Fig. 1** A). Hereafter, the term segment refers to a portion of the macromolecule between successive points of cross-links (**Fig. 1** A). N is assumed to be large (and it could vary for different types of macromolecules); L_0 would also not necessarily be same for all segments. Since the direction of each segment is a random variable, this confers a large number of conformations on the segment. However, the number of available conformations may be reduced further because of constraints, e.g. the molecules are connected ('network') at the points linking the segments of each molecule. Applying a statistical (mechanical) theory based on the elasticity of a network of (crosslinked) long-chain molecules (Treloar 1975) to model tissue deformation (Lepetit 2007), we derive the σ-ε equation for the case of a fascicle undergoing simple extension as follows. Let W represents the stored energy function, (i.e. arising from work done to cause an extension). Consider a segment of the macromolecule enclosed within an imaginary cube with the ends arbitrary fixed to the opposite faces of the cube (**Fig. 1** A). As the cube deforms the segment stretches (**Fig. 1** B). Let ζ_x, ζ_y and ζ_z represent the lengths (expressed in the form of extension ratios) of the deformed cube where subscripts *x, y* and *z* correspond to the respective axes of the Cartesian coordinate system (**Fig. 1** A, B). Thus, principal stresses act in the directions parallel to the principal axes of strain on planes corresponding to the faces of the deformed cube.

For simplicity, consider uniaxial tensile deformation in the direction of the *x* axis so that $\Sigma_y = \Sigma_z = 0$ (principal stresses at stress-free surfaces) and $\zeta_y = \zeta_z$. For comparison with the experimental data, we designate

$$\sigma = \Sigma_x / \zeta_x \tag{11}$$

to represent the nominal stress in the *x* axis direction; the corresponding nominal strain in the x axis direction is

$$\varepsilon = \zeta_x - 1 \tag{12}$$

(Defrate & Li 2007). Accordingly, the condition of constancy of volume (i.e. incompressibility)

$$\zeta_x \zeta_y \zeta_z = 1 \tag{13}$$

becomes

$$\zeta_y^2 = 1/\zeta_x. \tag{14}$$

We extend the argument for the single long segment to a network comprising of several macromolecules enclosed within a cube in ECM, in other words, a representative volume element of ECM. Given the entropy of each segment is associated with the number of conformations available, it follows that the entropy, *S*, of the macromolecular network in the volume element is the sum of the entropies of the segments. Let ΔS represents the change in *S* arising from *W*. We find

$$W = -T\Delta S, \tag{15}$$

to stretch the network elastically. As the starting point of our argument for quantifying the number of cross-link in the network, we note that

$$\Delta S = [-Nk/2]\{\zeta_x^2 + \zeta_y^2 + \zeta_z^2\}. \tag{16}$$

(A rigorous argument for the justification of this expression has been described by Treloar (1975) and no detailed recapitulation is appropriate here.) For the uniaxial tensile deformation in the *x* axis direction, substituting the expression for ζ_y in *Eq.* (14) into *Eq.* (16) leads to an intermediate expression $\Delta S = [-Nk/2]\{\zeta_x^2 + 2/\zeta_x\}$; subsequently, substituting the intermediate expression into *Eq.* (15) leads to

$$W = [NkT/2]\{\zeta_x^2 + 2/\zeta_x\}. \tag{17}$$

Differentiating *Eq.* (17) with respect to ζ_x leads to

$$\partial W/\partial\zeta_x = NkT\{\zeta_x - 1/\zeta_x^2\}. \tag{18}$$

Of note, both $\partial W/\partial\zeta_x$ and *W* are dimensionally similar (units, J/m^3). The work done by σ to cause a small change in ζ_x, i.e. $\delta\zeta_x$, is δW. By taking the limit of the $\delta W/\delta\zeta_x$, we find $\delta W/\delta\zeta_x \approx \partial W/\partial\zeta_x$ as $\delta\zeta_x$ becomes arbitrarily small. Since σ = $\partial W/\partial\zeta_x$, we can express σ in terms of ζ_x as follows

$$\sigma = NkT\{\zeta_x - 1/\zeta_x^2\}. \tag{19}$$

For practical implementation, we obtain *Eq*. (6) by substituting ε of *Eq.* (12) into *Eq.* (19) and evaluate the *G* from the experimental data points (σ, ε) by carrying out a regression analysis of *Eq*. (6) using the (σ, ε) data points from the origin to the yield point, which lies well within the range of small extensions (notably $\zeta_x < 2$) for which *Eq*. (19) is in good agreement with experimental data (Treloar 1975).

Appendix B Alternative arguments for computing ξ

In addition to the expression of ξ given by *Eq*. (5), it is worthwhile pointing out alternative arguments for computing ξ. Of note is a similar expression reported in an earlier study (David & Baeyens-Volant 1977). According to this study the UV energy absorbed per unit mass of the tissue is given by

$$\xi = c_\lambda \chi I_0 t, \tag{20}$$

where I_0 is now modelled by the UV intensity at the tissue surface, χ the specific volume, and c_λ the linear attenuation coefficient of the tissue. Although *t* is explicitly expressed in the equation, λ is implicitly implicated in I_0 and c_λ. Of note, in the original equation (David & Baeyens-Volant 1977), ξ and I_0 are expressed in units of the number of photons per unit gram and number of photons per unit square centimeter per unit minute, respectively. It follows that multiplying the photon number to the energy of a photon ($h\nu/\lambda$, where *h* is Planck's constant) leads to the unit

of Joules and so *Eq.* (5) is, in essence, dimensionally consistent with *Eq.* (20). We further note that the ρ/μ in *Eq.* (5) is dimensionally equivalent to $c_\lambda \chi$ in *Eq.* (20).

Spoerl et al. (2011) have offered a simple order of magnitude estimate for ξ. Consider UV (at a specified λ) emitting from a source of I_0 on an exposed surface area, ρ, of the specimen, for a predetermined t. Arguing that the transmitted intensity, I_r, through the tissue is of order of I_0, consequently, the product of I_0 with t is of the order of ξ.

Appendix C Logistic model

In this section, we describe a logistic approach to account for the accumulation of UV-induced crosslinks in the tissue, parameterizes by G, with increasing ξ, including the tipping point. Based on an analogy to the dynamics of chemical adsorption and desorption (Sadkowsi 2000) and oxidation kinetics (Hansford & Bailey 1992) we proposed a model to describe the increase in cross-links population with increases in ξ, constrain within a bounded system, i.e. the tissue, such that the growth would not continue indefinitely (unless we make changes to the parameters or boundaries of the system). This model is derived from a logistic differential equation which describes the growth rate, $\mathrm{d}G/\mathrm{d}\xi$, given by

$$\mathrm{d}G/\mathrm{d}\xi = G\{1-G/c_1\}/[c_1\Delta\xi]. \tag{21}$$

Here, on the right hand side of the *Eq.* (21), the G term is multiplied by a "negative feedback" factor, $\{1\text{-}G/c_1\}$, where c_1 is constant. The "negative feedback" factor contributes to slowing the growth rate as the limit c_1 is approached—the growth rate begins exponentially but then decreases to zero as the G approaches the limit c_1. Solving *Eq.* (21) analytically, we arrive at a solution given by *Eq.* (8) which describes

a sigmoidal profile, i.e. an S-shaped growth trajectory. For the purpose of fitting *Eq*. (8) to the experimental data of G versus ξ, the constant term, c_2, was introduced into *Eq*. (8) to account for the shift in the data along the G axis.

Appendix D Analysis of ξ in other studies

On the basis of the justification used to predict the values of the η, α, I_r, ρ/μ and ξ for the ACL model (section 3.3) and of Ω (section 4.2), we present a general strategy for application to the other studies (Table 1). In general, we note that I_0 is estimated as equal to the preset UV intensity and r as equal to the height of the chamber. Given the values of λ and t, step 1, substitute λ into *Eq*. (1) to determine η; step 2, determine α using *Eq*. (2) and the appropriate $A(\lambda)$ and $B(\lambda)$ (*Eq*. (3)); step 3, from the estimates of ρ and μ, determine ρ/μ; step 4, from the estimates of r and I_0, substitute (together with the values of η and α) into *Eq*. (6) to determine I_r; step 5, estimate Ω for UV-irradiated photosensitizer-impregnated tissue, otherwise proceed to next step; step 6, substitute I_r, ρ/μ and t into *Eq*. (7) to determine ξ—then multiply by Ω for photosensitizer-impregnated tissues to obtain the net energy absorbed per unit mass of the tissue specimen. As pointed out in section 4.2, for practical purpose—given G is not known but E is usually reported—we quantify Ω using E in place of G (which follows from the UV-stiffening hypothesis). Also, as there is no reference to the E of UV-irradiated photosensitizer-absent specimens in these instances, a conservative estimate places the E at equal to that of the controls. Finally, to estimate the t_C of UV irradiated photosensitizer-impregnated specimens, we use *Eq*. (5) to determine t_C (at $\xi = \xi_C$) for the photosensitizer-absent specimens, then divide by Ω (a correction

factor). In the following paragraphs, we present the arguments that led to the values of the key parameters used in our calculation of ξ for the other studies (Table 1).

For the RTT study of Sionkowska & Wess (2004), since RTTs are much larger than ACL fascicles, to order of magnitude, we set $\mu \approx 1\times10^{-4}$ g and $\rho \approx 0.0075$ cm^2. We thus find that $\rho/\mu \approx 75$ cm^2/g. We then apply the same argument for μ and ρ for the RTT study of of Fessel et al. (2012). However, for the EFT study (Fessel et al. 2012), our estimates of μ (≈ 1.0 g) and ρ (≈ 0.6 cm^2) are not unrealistic given the relatively larger size differences between the EFTs and the RTTs.

With reference to the RS study of Wollensak et al. (2005), the ratio of the mean *E* at *t* = 30 min to that of the (untreated) controls is 5.7; thus $\Omega \approx 5.7$. With a practical value of $\beta \approx 0.04$ g/cm^3 provided from measurements by Su et al. (2009), based on the size of the RS specimens it seems reasonable to take $\rho \approx 0.004$ cm^2. Multiplying β to the volume of a RS specimen (≈ 4.0×10.0×0.01 mm^3 = 4.0×10^{-3} cm^3) leads to $\mu \approx 4.0\times10^{-3}$ g. *Eq*. (5) predicts that $t_C \approx 68$ min (at $\xi = \xi_C$) for the photosensitizer-absent specimens; for photosensitizer-impregnated specimens, the critical time is $t_C/\Omega \approx$ 68/5.7 ≈ 12 min. For the HS study of Wollensak & Spoerl (2004), the ratio of the mean *E* at *t* = 30 min to that of the controls is approximately 1.3—thus $\Omega \approx 1.3$. Similarly, with a practical value of $\beta \approx 0.04$ g/cm^3 from measurements provided by Su et al. (2009), it seems reasonable to take $\rho \approx 0.32$ cm^2. Multiplying β to the volume of a HS specimen (≈ 4.0×8.0×2.0 mm^3 ≈ 6.4×10^{-2} cm^3) leads to $\mu \approx 2.6\times10^{-3}$ g. *Eq*. (5) predicts that $t_C \approx 8$ min (at $\xi = \xi_C$) for the photosensitizer-absent specimens; for photosensitizer-impregnated specimens, the critical time is $t_C/\Omega \approx$

8/1.3 ≈ 6 min. Thus the t (= 30 min) implemented in these studies are 3-5 times longer than the critical time.

For the PC study (Lanchares 2011), the ratio of the mean E at t = 30 min to the controls is approximately 1.4—thus $\Omega \approx 1.4$. (Note: for the specimen treated at t = 60 min, given there was no significant difference between the E at t = 60 min and those from the controls, we designate $\Omega = 1$.) Again, with a practical value of $\beta \approx 0.04$ g/cm^3 from measurements provided by Su et al. (2009), based on the size of the PC specimens it seems reasonable to take $\rho \approx 0.01$ cm^2. Multiplying β to the volume of a PC specimen (≈ 2.0×20.0×0.1 mm^3 = 4.0×10^{-3} cm^3) leads to $\mu \approx 1.6\times10^{-3}$ g. *Eq.* (5) predicts that $t_C \approx 15$ min (at $\xi = \xi_C$) for the photosensitizer-absent specimens; for photosensitizer-impregnated specimen, the critical time is $t_C / \Omega \approx 15/1.4 \approx 11$ min. Thus the t (= 30 min) implemented in the study is about 3 times longer than the critical time.

Additionally, we argue that the total energy absorbed by the tissue may be estimated to order of magnitude by multiplying the μ to the ξ. Apart from the EFT (Fessel et al. 2012) and RS (Wollensak et al. 2005) it follows that the total energy absorbed by the ACL specimens, and the tissues of other studies mentioned here are one to three orders of magnitude smaller than the limiting energy (≈ 3.4 J) known for causing cytotoxicity (Spoerl et al. 2011).

Appendix E Symbols

a_c Average cross-sectional area of a segment of the collagen macromolecule

A, B Polynomial functions of ultraviolet wavelength λ. Additionally, symbols a_i and b_i (i = 0, 1, 2...) represent constants of $A(\lambda)$ and $B(\lambda)$, respectively.

ACL Anterior cruciate ligament

c_2, c_2 Constants of the threshold model, *Eq.* (8)

c_λ Linear attenuation coefficient at a given ultraviolet wavelength λ

e Charge of electron

E Elastic modulus (stiffness) of the tissue; additionally, E_c represents the elastic modulus of collagen macromolecule

ECM Extracellular matrix

EDT Equine superficial digital flexor tendon

F Force on an individual segment of collagen macromolecule

G Thermodynamic shear-related parameter; additionally, ΔG represents the difference between the maximum (G_{max}) and minimum (G_{min}) G

HS Human sclera

I_0 Ultraviolet source intensity

I_r Ultraviolet intensity at distance, r, from the source

L_0 Average length of a segment of the collagen macromolecule

m_e Mass of electron

M Average molecular mass of a segment of the collagen macromolecule

N Number of collagen macromolecular segments per unit volume of ECM involved in the deformation of the tissue

N_A Avogadro's constant

PC Porcine cornea

PG Proteoglycan

r Pathlength of ultraviolet photon

RTT Rat tail tendon

S Entropy; additionally ΔS refers to the change in entropy

SEM Scanning electron microscopy

T Absolute temperature; additionally, T_0 represents the reference temperature

t Ultraviolet exposure time; additionally, Δt refers to the duration of increase from G_{min} to G_{max}

t_C Critical t

U Displacement of a segment of the collagen macromolecule

UV Ultraviolet light

u_Y Modulus of resilience of the tissue

v speed of light

W Work of elastic deformation

x, y, z Axes of the Cartesian coordinate system

α Molecular absorption cross-sectional area

β Tissue density

χ Specific volume

ε Nominal strain

ε_Y Yield ε of the tissue

Ω Radiomechanical photosensitizer efficiency

κ Permittivity of the medium (connective tissue)

η Electron density of the micro-environment in connective tissue

λ UV wavelength

ρ / μ Specific surface area, defined as the ratio of exposed surface area (ρ) to the mass of the specimen (μ)

σ Nominal stress

$\Sigma_x, \Sigma_y, \Sigma_z$ Stress components in the direction of the respective Cartesian coordinate axes

σ_Y Yield σ of the tissue

ξ UV photon energy per unit mass absorbed by the tissue

ξ_C Critical ξ for the formation of covalent cross-links

ξ_D Threshold level of ξ above which chain scission predominates

$\zeta_x, \zeta_y, \zeta_z$ Extension ratios in the direction of the respective Cartesian coordinate axes

Acknowledgements

Support for this work was provided by grants from the Ministry of Education, Singapore (AcRF 34/06).

References

1. Bailey AJ (2001) Molecular mechanisms of ageing in connective tissues. Mechanisms of Ageing and Development 122:735–755

2. Balmer RT (1982) The effect of age on body energy content of the annual cyprinodont fish, Nothobranchius Guentheri. Experimental Gerontology 17:139-143

3. Buehler MJ (2006) Nature designs tough collagen: Explaining the nanostructure of collagen fibrils. Proceedings of the National Academy of Sciences USA 103: 12285–12290

4. Chan BP (2010) Biomedical applications of photochemistry. Tissue Engineering Part B 16:509-522

5. Charlesby A (1977) Use of high energy radiation for crosslinking and degradation. Radiation Physics and Chemistry 9:17-29

6. Charlesby A (1981) Crosslinking and degradation of polymers. Radiation Physics and Chemistry 18:59-66

7. David C, Baeyens-Volant D (1978) Statistical theories of main chain scission and crosslinking of polymers – application to the photolysis and radiolysis of polystyrene studied by gel permeation chromatography. European Polymer Journal 14:29-38

8. Derwin KA, Soslowsky LJ (1999) A quantitative investigation of structure-function relationships in a tendon fascicle model. Journal of Biomechanical Engineering 121:598-604

9. DeFrate IE, Li G (2007) The prediction of stress-relaxation of ligaments and tendons using the quasi-linear viscoelastic model. Biomechanics and Modeling in Mechanobiology 6:245–251

10. Fessel G, Snedeker JG (2009) Evidence against proteoglycan mediated collagen fibril load transmission and dynamic viscoelasticity in tendon. Matrix Biology 28:503–510

11. Fessel G, Wernli J, Li Y, Gerber C, Snedeker JG (2012) Exogenous collagen cross-linking recovers tendon functional integrity in an experimental model of partial tear. Journal of Orthopedic Research 30:973–981

12. Fisher BT, Hahn DW (2004) Measurement of small-signal absorption coefficient and absorption cross section of collagen for 193-nm excimer laser light and the role of collagen in tissue ablation. Applied Optics 43:5443-5451

13. Fujimori E (1966) Ultraviolet light irradiated collagen macromolecules. Biochemistry 5:1034-1040

14. Goh KL, Meakin JR, Aspden RM, Hukins DWL (2005) Influence of fibril taper on the function of collagen to reinforce extracellular matrix, Proceedings of the Royal Society of London B 272:1979–1983

15. Goh KL, Holmes DF, Lu HY, Richardson S, Kadler KE, Purslow PP, Wess TJ (2008) Ageing changes in the tensile properties of tendons: influence of collagen fibril volume fraction. Journal of Biomechanical Engineering 13:021011

16. Goh KL, Holmes DF, Lu Y, Purslow PP, Kadler KE, Bechet D, Wess TJ (2012) Bimodal collagen fibril diameter distributions direct age-related variations in

tendon resilience and resistance to rupture. Journal of Applied Physiology 113:878-888

17. Gautieri A, Buehler MJ, Redaelli A (2009) Deformation rate controls elasticity and unfolding pathway of single tropocollagen molecules. Journal of the Mechanical Behaviour of Biomedical Materials 2:130–137

18. Hansford GS, Bailey AD (1992) The logistic equation for modelling bacterial oxidation kinetics. Minerals Engineering, 5: 1355-1364

19. Hirokawa S, Sakoshita T (2003) An experimental study of the microstructure and mechanical properties of swine cruciate ligaments. JSME International Journal Series C 46:1417-1425

20. Kadler KE, Baldock C, Bella J, Boot-Handford RP (2007) Collagen at a glance. Journal of Cell Science 120: 1955-1958

21. Khoshgoftar M, Wilson W, Ito K, van Donkelaar CC (2012) Influence of tissue- and cell-scale extracellular matrix distribution on the mechanical properties of tissue-engineered cartilage. Biomechanics and Modeling in Mechanobiology DOI 10.1007/s10237-012-0452-1

22. Lanchares E (2011) Biomechanical property analysis after corneal collagen cross-linking in relation to ultraviolet A irradiation time. Graefe's Archive for Clinical and Experimental Ophthalmology 249:1223–1227

23. Lepetit J (2007) A theoretical approach of the relationships between collagen content, collagen cross-links and meat tenderness. Meat Science 76:147-159

24. Lewis PN, Pinali C, Young RD, Meek KM, Quantock AJ, Knupp C (2010) Structural interactions between collagen and proteoglycans are elucidated by three-dimensional electron tomography of bovine cornea. Structure 18, 239–245

25. Meller R, Moortgat GK (1997) CF3C(O)CI: Temperature-dependent (223-298 K) absorption cross-sections and quantum yields at 254 nm. Journal of Photochemistry and Photobiology A: Chemistry 108:105-116

26. Miles CA, Sionkowska A, Hulin SL, Sims TJ, Avery NC, Bailey AJ (2000) Identification of an intermediate state in the helix-coil degradation of collagen by ultraviolet light. Journal of Biological Chemistry 275:33014–33020

27. Orgel JPRO, San Antonio JD, Antipova1 O (2011) Molecular and structural mapping of collagen fibril interactions. Connective Tissue Research 52: 2–17

28. Quinn TM, Morel V (2007) Microstructural modeling of collagen network mechanics and interactions with the proteoglycan gel in articular cartilage. Biomechanics and Modeling in Mechanobiology 6:73–82

29. Rabotyagova OS, Cebe P, Kaplan DL (2008) Collagen structural hierarchy and susceptibility to degradation by ultraviolet radiation. Material Science and Engineering C 28:1420–1429

30. Redaelli A, Vesentini S, Soncini M, Vena P, Mantero S, Montevecchi FM (2003) Possible role of decorin glycosaminoglycans in fibril to fibril force transfer in relative mature tendons—a computational study from molecular to microstructural level. Journal of Biomechanics 36:1555-1569

31. Rigozzi S, Muller R, Stemmerb A, Snedeker JG (2013) Tendon glycosaminoglycan proteoglycan sidechains promote collagen fibril sliding—AFM observations at the nanoscale. Journal of Biomechanics 46:813-818

32. Sadkowsi A (2000) On the application of the logistic differential equation in electrochemical dynamics. Journal of Electroanalytical Chemistry 486:92-94

33. Samoria C, Valles E (2004) Model for a scission-crosslinking process with both H and Y crosslinks. Polymer 45:5661-5669

34. Scott JE (2003) Elasticity in extracellular matrix 'shape modules' of tendon, cartilage, etc. A sliding proteoglycan-filament model. Journal of Physiology 553:335-343

35. Sionkowska A, Wess TJ (2004) Mechanical properties of UV irradiated rat tail tendon (RTT) collagen. International Journal of Biological Macromolecules 34:9-12

36. Spoerl E, Hoyer A, Pillunat LE, Raiskup F (2011) Corneal cross-linking and safety issues. Open Ophthalmology Journal 5:14-16

37. Su X, Vesco C, Fleming J, Choh V (2009) Density of ocular components of the bovine eye. Optometry & Vision Science 86:1187-1195

38. Thyagarajan M, Scharer J (2008) Experimental investigation of ultraviolet laser induced plasma density and temperature evolution in air. Journal of Applied Physics 104:013303

39. Thornton HG (1922) On the development of a standardized agar medium for counting soil bacteria. Annals of Applied Biology 9:241–74

40. Treloar LRG (1975) The physics of rubber elasticity, 3rd edn. Clarendon Press, Oxford

41. Wollensak G, Spoerl E (2004) Collagen crosslinking of human and porcine sclera. Laboratory Science 30:689-695

42. Wollensak G, Iomdina E, Dittert D-D, Salamatina O, Stoltenburg G (2005) Cross-linking of scleral collagen in the rabbit using riboflavin and UVA. Acta Ophthalmologica Scandinavica 83:477–482

Figure captions

Fig. 1 Schematics of a segment of collagen macromolecule in extracellular matrix before deformation (A) and after deformation (B). Inset in A (figure to the left) is a schematic of staggered axial packing of collagen macromolecules bound by cross-links. Graph in C shows typical stress (σ) versus strain (ε) curves of ligament fascicles from the control group and the ultraviolet light (UV) treated group (wavelength, 365 nm; exposure time, 30 min). Symbols: ○, control group; □, the UV treated group. Both curves feature the following regions: toe, near-linear elastic, plastic and fracture; these regions are typical of ligament and tendon fascicles. The transition from elastic to plastic is indicated by the point Y; point M indicates the state of maximum stress; a dramatic decrease in the stress occurs thereafter and eventually the fascicle breaks into two (point F).

Fig. 2 Ligament fascicles. Optical micrographs of fascicles (A) before loading and (B) rupture at post-peak stress; scanning electron micrographs (SEMs) of the fascicle morphology (C) before loading and (D) at rupture. Insets in A-B are the magnified views of the fascicle; horizontal (scale) bar has a length of 100 mm. Arrows b and f in C-D point to fibril bundles and individual fibrils; SEM magnification, ×1500.

Fig. 3 Plots of interaction and main effects of ultraviolet wavelength, λ, and exposure time, t, of the respective ligament fascicle parameters: thermodynamic shear-related parameter, G, stiffness (E) and modulus of resilience, u_Y. Left subpanels: interaction plots; right subpanels: main effects. * $P < 0.05$, ** $P < 0.01$. Number of specimens analysed: λ = 254 nm, 13 (15 min), 12 (30 min), 12 (60 min); at λ = 365 nm, 12 (15 min), 14 (30 min), 14 (60 min).

Fig. 4 Graphs of (A) absorbed ultraviolet (UV) energy, ξ, per unit mass of the tissue versus exposure time, *t*, and (B) thermodynamic shear-related parameter, *G*, versus ξ for ligament fascicles, at the level of λ = 365 nm. *Eq.* (5) was used to derive the plot in A; t_C and ξ_C represent the critical *t* and ξ, respectively. In B, the threshold model, *Eq.* (8), was fitted to the data points from the controls and UV 365 nm group. Solid line, $\Delta\xi$ = 1.3 J/g; dashes $\Delta\xi$ = 2.2 J/g. G_{min} = 63.1 MPa; G_{max} = 130.1 MPa. Mean ± standard error of the mean in (B)

Fig. 5 Box-and-whisker plots of the ligament fascicle (A) elastic modulus, *E*, and (B) modulus of resilience, u_Y, at the G_{min} and G_{max} derived using data from the controls and UV 365 nm group. Median (horizontal line); 25 % and 75 % percentile (box); 5 % and 95% percentile (whisker ends); white circles represent the mean value.

Figures

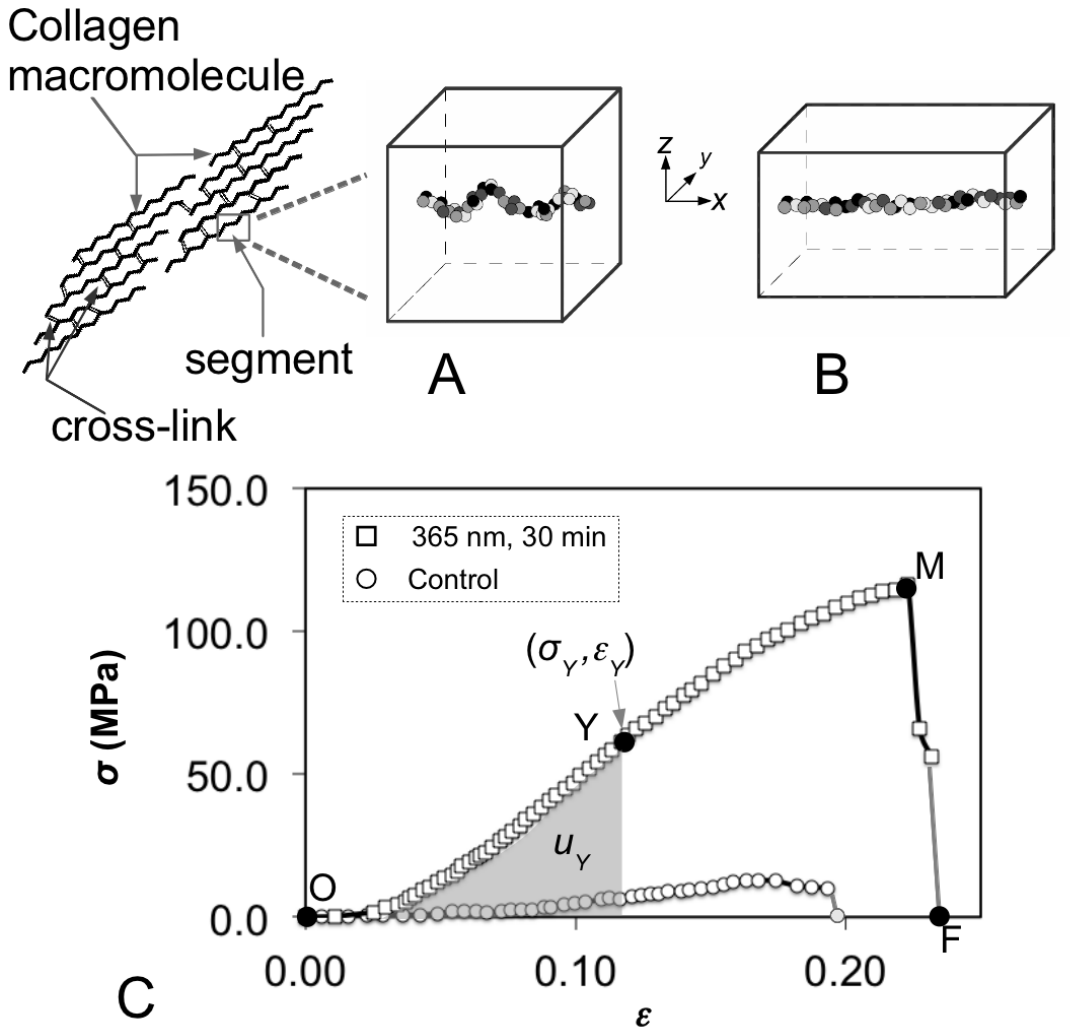

Fig. 1

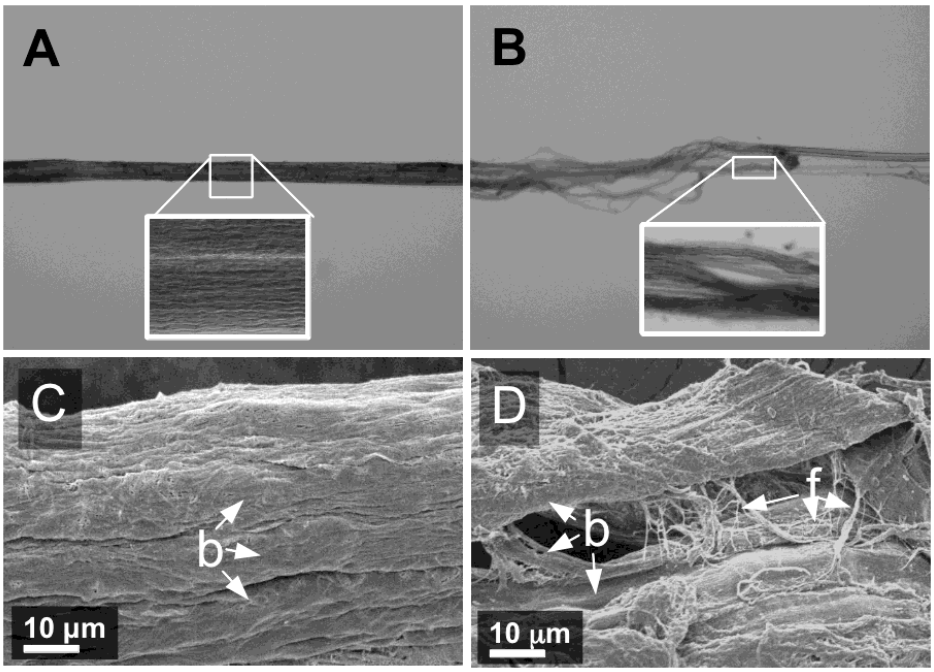

Fig. 2

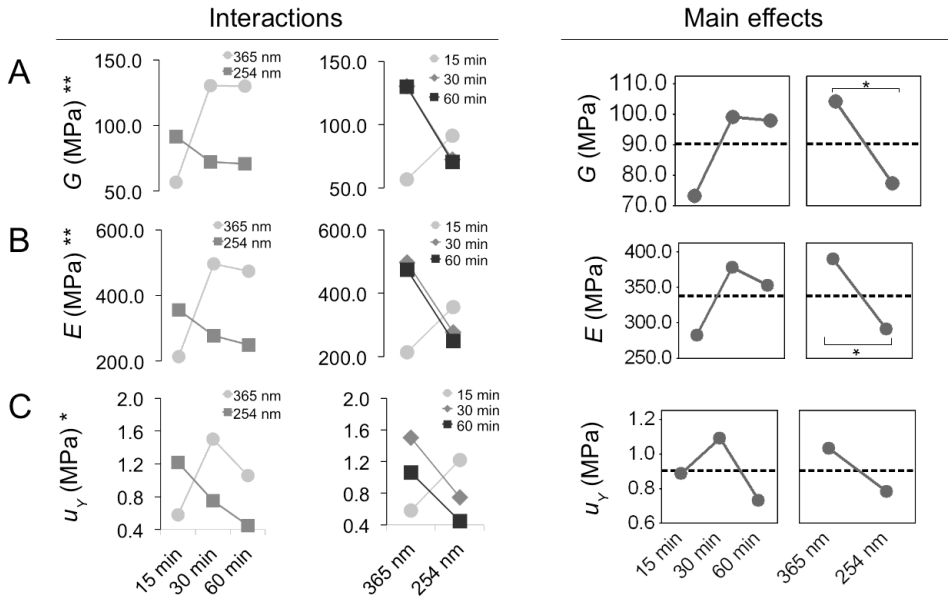
Interactions
Main effects
A
B
C
G (MPa) **
E (MPa) **
u_Y (MPa) *
365 nm
254 nm
15 min
30 min
60 min
150.0
100.0
50.0
600.0
400.0
200.0
2.0
1.6
1.2
0.8
0.4
110.0
100.0
90.0
80.0
70.0
400.0
350.0
300.0
250.0
1.2
1.0
0.8
0.6
*

Fig. 3

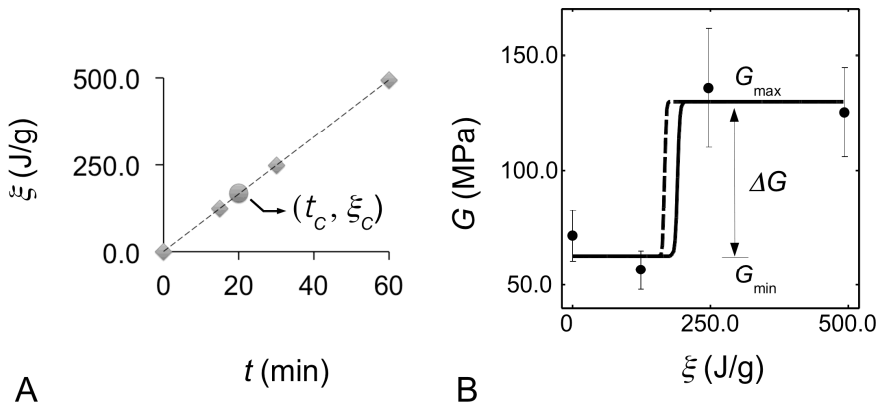
500.0
250.0
0.0
ξ (J/g)
0
20
40
60
t (min)
(t_c, ξ_c)
A
150.0
100.0
50.0
G (MPa)
G_max
ΔG
G_min
0
250.0
500.0
ξ (J/g)
B

Fig. 4

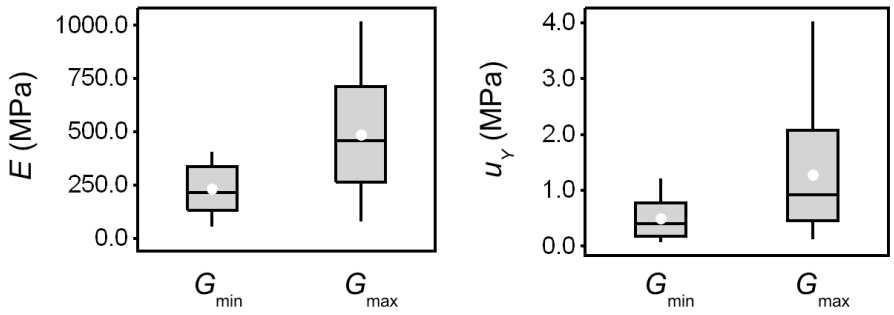
E (MPa)
1000.0
750.0
500.0
250.0
0.0
G min
G max
u y (MPa)
4.0
3.0
2.0
1.0
0.0
G min
G max

Fig. 5